ELSEVIER

Biophysical Chemistry 116 (2005) 11–21

Biophysical Chemistry

http://www.elsevier.com/locate/biophyschem

Comparison of the helix–coil transition of a titrating polypeptide in aqueous solutions and at the air–water interface

Helen Sjögren[a,1], Stefan Ulvenlund[a,b,*]

[a]*Physical Chemistry 1, Lund University, P.O. Box 124, 221 00 Lund, Sweden*
[b]*AstraZeneca R&D Lund, 221 87 Lund, Sweden*

Received 3 December 2004; received in revised form 18 January 2005; accepted 18 January 2005
Available online 29 January 2005

Abstract

The transition from α-helix to random coil of the titrating polyamino acid co-poly-L-(lysine, phenylalanine), (p-(Lys,Phe)), has been investigated as a function of pH and ionic strength in aqueous solution and at the air–water interface by means of circular dichroism (CD) spectroscopy and the Langmuir surface film balance technique. The results strongly suggest that the helix–coil transition for peptides at the air–water interface can be determined by using the two-dimensional Flory exponent, ν, to express the pH dependent peptide surface conformation. The helix–coil titration curve of p-(Lys,Phe) shifts approximately 2.5 pH units towards lower pH at the air–water interface, as compared with the bulk solution. This finding is of relevance for the understanding of conformation and conformational changes of membrane-transporting and membrane penetrating peptides as well as for the use of peptides in molecular devices.

Keywords: Polyamino acid; Molecular monolayer; Compression isotherm; Flory exponent; α-helix to random coil transition; Langmuir–Blodgett film

1. Introduction

Helix-to-coil transitions are ubiquitous to biological macromolecules, and are often of decisive importance for their biological function. However, the sheer complexity of native systems often calls for studies of simpler, synthetic model compounds. Over the years, polymers and co-polymers of α-L-amino acids (polyamino acids) have been extensively studied in aqueous solutions, in order to understand the behaviour of native peptides. The use of polyamino acids as peptide models builds on the observation that peptide function in vivo is intimately linked to dynamic changes between different conformations, and that quite simple peptides may act as powerful models for the ordered conformations in the more complicated systems [1]. Studies of polyamino acids have thus provided detailed insight into the aggregation behaviour of peptides [2] and the dependence of peptide secondary conformation and conformation stability on temperature and solvent characteristics [3–10].

Studies of poly-L-lysine (p-Lys) and poly-(L-lysine, phenylalanine) (p-(Lys,Phe)), interactions with membranes have shown that peptide secondary conformation directly influences membrane diffusion or permeability [11,12], and that an increased amount of α-helical conformation facilitates peptide penetration into vesicle bilayers [13]. Similarly, the polyamino acids have helped elucidate the mechanism of membrane-transporting peptides, which transport macromolecules like DNA and proteins through cell membranes [14]. The trans-membrane DNA transport mediated by p-Lys and p-(Lys,Phe) involves formation of complexes between the polyamino acid and DNA [14,15]. These complexes have found use as non-viral vectors for gene delivery used in treatment of, for instance, cancer and cystic fibrosis [16–18]. Both p-Lys and p-(Lys,Phe) are also known to possess fusogenic activity, i.e. to induce vesicle

* Corresponding author. AstraZeneca R&D Lund, 221 87 Lund, Sweden. Fax: +46 46 337128.
E-mail addresses: Helen.Sjogren@fkem1.lu.se (H. Sjögren), Stefan.Ulvenlund@astrazeneca.com (S. Ulvenlund).
[1] Née Gillgren.

0301-4622/$ - see front matter © 2005 Elsevier B.V. All rights reserved.
doi:10.1016/j.bpc.2005.01.007

fusion. Studies of the fusion process have been claimed to help the understanding of complex biological processes such as endo-and exocytosis, fertilisation and formation of myofibrils, which involve biological membrane fusion [19]. Interaction between p-(Lys,Phe) and vesicles induces changes in the polyamino acid secondary peptide conformation, yielding more α-helix conformation [20].

All of the above applications and phenomena actually involve surface processes, and it is therefore of obvious importance to understand peptide behaviour not only in solution, but also at interfaces. In particular, it is important to understand the differences between helix-to-coil transitions in solution and those at interfaces. Peptide and protein conformation and conformational changes at the air–water have previously been investigated [21,22]. For example, β-casein has been studied at the surface of different aqueous solutions [23–26]. However, there seem to be no previous studies that directly compare the helix-to-coil transition of a given peptide in solution with that at the air–water surface. For this reason, we have investigated the helix-to-coil transition for p-(Lys,Phe) in aqueous solution, as well as on the air–water interface, under conditions where solution pH and ionic strength are rigorously controlled. Despite the large numbers of studies already performed on p-(Lys,Phe), a detailed study of its pH dependent helix–coil transition is still lacking. The present work is therefore also of direct relevance for the numerous technical applications of this peptide.

2. Materials and methods

2.1. Chemicals

Co-poly-L-(lysine, phenylalanine) HBr (p-(Lys,Phe)) and poly-L-lysine HCl (p-Lys) were purchased from Sigma Chemicals. They were stored at −18 °C and used as received. The mean molecular weight (M_w) stated by the manufacturer is 49 kDa for p-(Lys,Phe) and 52.5 kDa for p-Lys, both determined by viscosimetry. This corresponds to an average degree of polymerisation of 275 and 319, respectively. In p-(Lys,Phe) the Lys:Phe molar ratio stated by the manufacturer is 52:48. Dichloromethane of spectrophotometric grade was obtained from Aldrich. Trifluoracetic acid (TFA) of Uvasol® grade was obtained from Merck. Both solvents were used as received. The absence of surface active contaminants in the solvents was verified by spreading the neat solvents on clean water in the surface balance trough and then, after 15 min, recording the surface pressure upon compression. The solvents were found not to affect the surface pressure at any degree of compression relevant for the present study.

n-Dodecyl-β-D-maltoside (β-$C_{12}G_2$) was obtained from Anatrace Inc. and was of Anagrade™ quality. Acetic acid, NaCl and sodium acetate of p.A. grade, as well as HCl and NaOH of Titrisol® grade were purchased from Merck. Trizma® base of SigmaUltra quality was purchased from Sigma and sodium hydrogen carbonate of p.A. grade was purchased from Fluka. Distilled water was purified on a PureLab Plus water purification apparatus. The water had an electrical resistivity of >18 MΩ/cm and was filtered through a 0.10-μm filter prior to experiments.

2.2. Preparation of buffer solutions

All solutions used as subphases in the surface experiments had a buffer concentration of 0.05 M. Appropriate amounts of NaCl were added, to give an ionic strength of either 0.1 or 0.5 M, irrespective of pH. Buffer solutions used for experiments with p-(Lys,Phe) in aqueous solutions had a buffer concentration of 0.02 M, and the ionic strength was kept constant at either 0.02 or 0.1 M by addition of NaCl. Depending on the pH range under study, either acetate, tris or carbonate buffer was used. For all titration curves (both in bulk and on surfaces) an overlap of at least one pH unit was used when switching buffer system, in order to check for buffer dependent effects. No such effects were observed. The range of salt concentrations possible to investigate is, at low ionic strength, limited by the requirement to have a high enough buffer concentration to prevent drift in pH and, at high ionic strength, by the requirement that the level of background UV absorption in CD measurements must be kept sufficiently low.

2.3. Preparation of spreading solutions

The solid p-(Lys,Phe) used in this work was found to be insoluble in all common organic solvents, except TFA and mixtures of TFA and dichloromethane with a maximum TFA:dichloromethane ratio of 1:5. Spreading solutions were therefore prepared by first dissolving p-(Lys,Phe) in pure TFA and thereafter dilute this solution by dichloromethane to a TFA:dichloromethane ratio of 1:5. The p-(Lys,Phe) concentration used in the final TFA:dichloromethane spreading solutions in all surface balance experiments was 1 mg/ml.

2.4. Formation of polymer films and recording of isotherms

Isotherms were recorded on a KSV 2000 System 2 surface balance equipped with hydrophilic barriers, a Wilhelmy plate made of roughened platinum and a thermostatted Teflon trough with a total surface area of 510×150 mm (765 cm^2). The trough was thermostatted at 25.0 °C by means of a circulating water bath and enclosed in a Plexiglas box in order to avoid airborne contaminants. The Wilhelmy plate was oriented roughly parallel to the barriers. The surface was cleaned prior to the spreading of a polymer film on the subphase as described elsewhere [27]. 50 μl of the spreading solution was added to the clean subphase surface by careful, drop-wise additions from a Hamilton syringe and the solvent allowed to evaporate for at

least 15 min prior to compression. The film was then symmetrically and continuously compressed. All isotherms were recorded using a barrier speed of 10 mm/min.

A given subphase was used for a maximum of four experiments before being discarded. The pH of the subphase was monitored with a Metrohm 744 pH meter after each isotherm experiment. The pH of the subphase was found to decrease 0.2 pH units or less over a series of four experiments. However, this decrease did not affect the isotherms. In the following, the *mean molecular area* is denoted A_0 and given as calculated per amino acid residue.

2.5. Deposition of Langmuir-Blodgett (LB) films

Prior to LB deposition, the film under study was compressed beyond the target surface pressure, 18 mN m^{-1}, then decompressed and kept at the target pressure for at least 20 min. Deposition was then performed by raising the substrate through the film at a speed of 3 mm/min. The substrate was oriented parallel to the barriers. All transfer ratios were in the range 0.96–1.08.

For analysis by atomic force microscopy (AFM), plates of freshly cleaved mica were used as substrates in the LB deposition. LB films for analysis by circular dichroism (CD) spectroscopy were deposited on rectangular plates (50×12 mm) of optic quartz. Prior to the deposition, the plates were placed in sulphochromic acid for several hours and then washed with large amounts of purified water.

2.6. Circular dichroism spectroscopy

CD spectra of aqueous solutions and LB films of polyamino acid were recorded on a Jasco J715 spectropolarimeter. For LB films, the quartz plate supporting the film was placed in the standard cuvet holder of the instrument. Two perpendicular orientations of the quartz plate were investigated in order to check for contributions from linear dichroism originating from long-range net lateral orientation of the polyamino acid strands on the substrate. Due to the weak CD signal from the LB films, over-night sampling (corresponding to >700 scans) was required. The low intensity of the signal also necessitated correction for the weak background contribution from the quartz substrate and minor instrument misalignment. Consequently, the CD signal from a clean quartz plate was recorded by over-night sampling and this signal was subsequently subtracted from all spectra of LB films.

Aqueous solutions analysed by CD spectroscopy had a polyamino acid unimer concentration of 0.15 mM and were enclosed in a 10 mm quartz cuvet. All measurements were performed at 25.0 °C within 1 h from sample preparation. The CD signal recorded at 225 nm was used in calculations of the polyamino acid conformation. However, the CD spectra were scanned between 220 and 250 nm to verify absence of other secondary conformations than α-helix and random coil. The ratio of helix and coil was calculated by assuming that the measured CD signal depends linearly on this ratio. P-(Lys,Phe) and p-Lys forms only α-helical and/or random coil conformation under the conditions used in the present study. The recorded CD signal, A, can thus be expressed as

$$A = A_\alpha X_\alpha + (1 - X_\alpha)A_c \quad (1)$$

where A_α and A_c is the CD signal for a peptide in a 100% α-helix and a 100% random coil conformation, respectively, whereas X_α is the fraction of the peptide conformation in α-helical conformation. Eq. (1) can be rewritten as

$$X_\alpha = (A - A_c)/(A_\alpha - A_c) \quad (2)$$

For p-Lys, conditions for obtaining 100% α-helix or 100% random coil conformation can be found in the literature. At 22 °C, 0.01–0.06% solutions of p-Lys at pH≤5 are known to form a 100% random coil conformation, whereas the same p-Lys concentration form a 100% α-helix conformation at pH≥11 [28]. In this study a 0.15 mM (unimer concentration) p-Lys solution in 0.1 M HCl and 0.1 M NaOH was used for determine the 100% random coil and 100% α-helix spectra, respectively. As will be discussed in more detail in the Results section, p-(Lys,Phe) contains appreciable amounts of α-helix in 0.1 M HCl solutions due to high ionic strength of such solutions. For p-(Lys,Phe), a spectra corresponding to a 100% random coil conformation was instead observed in 0.02 M acetic acid solution. Conditions for formation of 100% helix was achieved in a 0.1 M NaOH solution containing 5 mM of β-$C_{12}G_2$. The addition of surfactant was found necessary in order to inhibit precipitation of the peptide.

2.7. Atomic force microscopy

Constant force AFM studies of LB films on mica were performed in contact mode on a Nanoscope® IIIa instrument (Digital Instruments, Santa Barbara, CA). Experiments were run under ambient atmosphere and temperature within 10 h from sample preparation. An E tube scanner was used for imaging. Microfabricated square pyramidal shaped tips of silicon nitride with a bending spring constant of 0.12 N/m (manufacture specified, Digital Instruments, Santa Barbara, CA) were used as received. The scan rate was 2 Hz and the applied force was in the order of 1–10 nN. Each sample was checked for tip-induced damages after scanning. The samples were scanned in two directions perpendicular to each other to secure that the image was not influenced by the scanning direction.

Images were obtained from at least ten macroscopically separated areas on each sample. All images were processed using standard procedures for plane-fit and flattening in Nanoscope® IIIa software version 5.12 (Digital Instruments, Santa Barbara, CA) without any filtering.

3. Results and discussion

3.1. P-(Lys,Phe) in aqueous solutions

The CD signal of aqueous p-(Lys,Phe) solutions measured at 225 nm as a function of pH displays a drastic decrease when the pH is increased, consistent with a transition from random coil to α-helix (Fig. 1). This pH dependent transition has both entropic and enthalpic origins. Increasing the pH decreases the number of charges on the p-(Lys,Phe) peptide (pK_a for lysine in solution is 10.53) [29], and hence decreases the electrostatic repulsion between the polyamino acid unimers. In addition, the entropic loss of counter-ion binding vanishes when the polyamino acid is neutralized (increased pH) and the counterions are released to the surrounding solution. A decreased polyamino acid net charge thus favours α-helix formation for both entropic and enthalpic reasons, but it also lowers the polyamino acid water solubility. Consequently, p-(Lys,Phe) was observed to precipitate from solutions above pH 9.5, unless a solubilising agent is added. The non-ionic surfactant β-$C_{12}G_2$ was found to act as such an agent. It stabilises the α-helical conformation, prevents precipitation and thereby enables the whole titration curve to be determined (Figs. 1 and 2).

Since the complete titration curve for p-(Lys,Phe) could not be determined in the absence of surfactant, a direct comparison between the behaviour of p-Lys and p-(Lys,Phe) is not possible over the whole pH range (Fig. 2). However, since the titration curve of p-(Lys,Phe) with addition of β-$C_{12}G_2$ yields a titration curve that only shows a parallel shift compared with the system without surfactant (Fig. 2), the titration curves of p-Lys and p-(Lys,Phe) can be compared in qualitative terms.

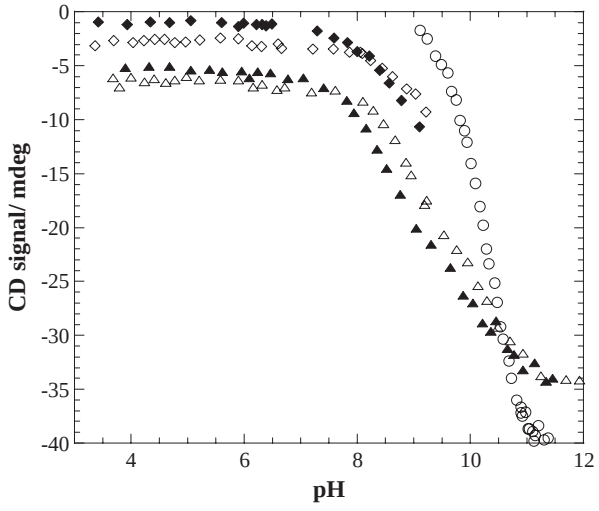

Fig. 1. CD signal at 225 nm as a function of pH for p-(Lys,Phe). The ionic strength was kept constant at 0.02 M (filled symbols) and 0.1 M (open symbols) by addition of NaCl. The titration curve for p-(Lys,Phe) was measured with (triangles) and without (diamonds) addition of 5 mM β-$C_{12}G_2$. The titration curve for p-Lys (circles) is added for comparison.

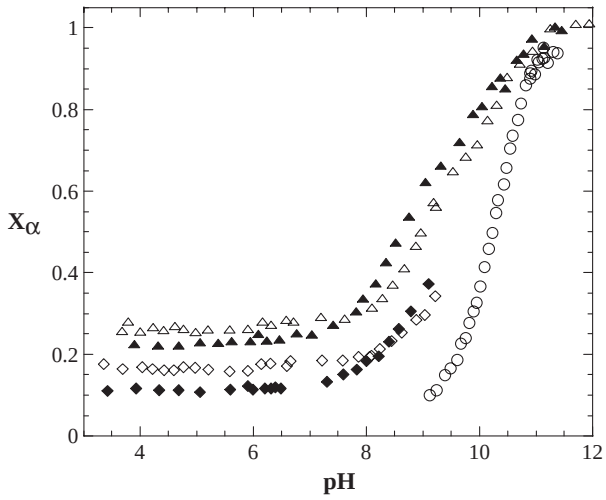

Fig. 2. X_α (calculated from Eq. (2)) as a function of pH for p-(Lys,Phe). The ionic strength was kept constant at 0.02 M (filled symbols) and 0.1 M (open symbols) by addition of NaCl. The titration curve for p-(Lys,Phe) was measured with (triangles) and without (diamonds) addition of 5 mM β-$C_{12}G_2$. The titration curve for p-Lys (circles) is added for comparison.

In comparison to p-Lys, the helix-to-coil transition of p-(Lys,Phe) is broadened and shifted towards lower pH. Adding β-$C_{12}G_2$ shifts the transition further towards lower pH, but does not appear to have any impact on the width of the helix-to-coil transition (Fig. 2). Addition of β-$C_{12}G_2$ to p-(Lys,Phe) yields at least 10% more α-helix conformation, at any given pH, in the whole region where measurements could be performed. Adding β-$C_{12}G_2$ to p-Lys on the other hand, does not give rise to an increase of α-helix content in any part of the titration curve (result not shown).

The effect of the ionic strength on the α-helix content in p-(Lys,Phe) does not depend on whether β-$C_{12}G_2$ addition is made or not (Fig. 2). At low pH (≤8) an increased ionic strength increases the amount of polyamino acid in α-helical conformation. This is easily understood from the fact that an increased salt concentration decreases the electrostatic repulsion between charged lysine monomers and decreases the entropic loss of counterion condensation, which both facilitate α-helix formation. At higher pH, on the other hand, an increase in ionic strength yields a decease in the amount of polyamino acid in α-helix conformation. This observation is, as yet, not fully understood and common theoretical models used to predict peptide secondary conformation fail to account for this salt dependence [30]. However, a possible explanation could be the subtle shift of the balance between the free energy of electrostatic interaction between side-chains (where an increased ionic strength favours α-helix formation) and the free energy contribution arising from the fact that the charge density of the peptide as a whole is not independent of the salt concentration in this pH region. More specifically, the increase of the charge density with salt addition is more pronounced for the α-helix conformation, which means that an increased ionic strength actually favour random coil formation [31,32].

3.2. P-(Lys,Phe) at the air–water interface

Despite the fact that p-(Lys,Phe) is soluble in the buffer solutions up to pH 9.5 it forms remarkably stable monolayers when spread at the air–water interface on subphases with pH≥3.5 (Fig. 3). The surface pressure isotherms display good reproducibility under all pH conditions, as exemplified in Fig. 3. In addition, the surface pressure isotherms upon repeated compression and decompression cycling display only minute loss of material to the subphase when the films were compressed up to 47 mN m^{-1} (normally less than 5% after three compression/decompression cycles). However, at compression to higher surface pressures, Π>47 mN m^{-1}, film material is irreversible lost to the subphase, barriers and trough walls (results not shown). Even at extremely low pH and ionic strengths (pH=3 and I=1 mM) only less than 10% of the monolayer material is lost after two repeated compression and decompression cycles (results not shown).

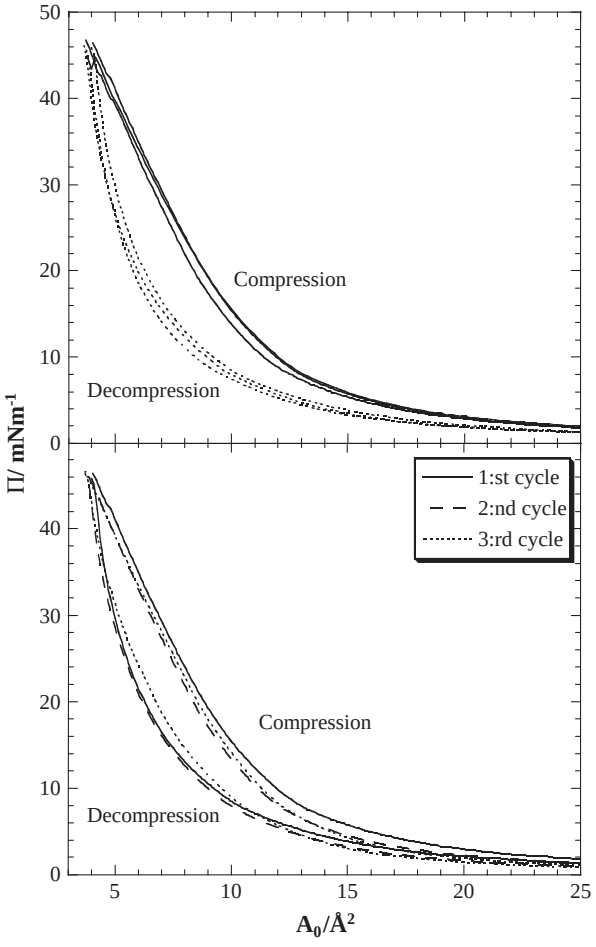

Fig. 3. Surface pressure isotherms of p-(Lys,Phe) spread on 0.1 M acetate buffer pH 3.7. Upper figure shows compression (solid trace) and decompression (dotted trace) isotherms from three independent measurements. Lower figure shows the isotherms of three repeated compression/decompression cycles.

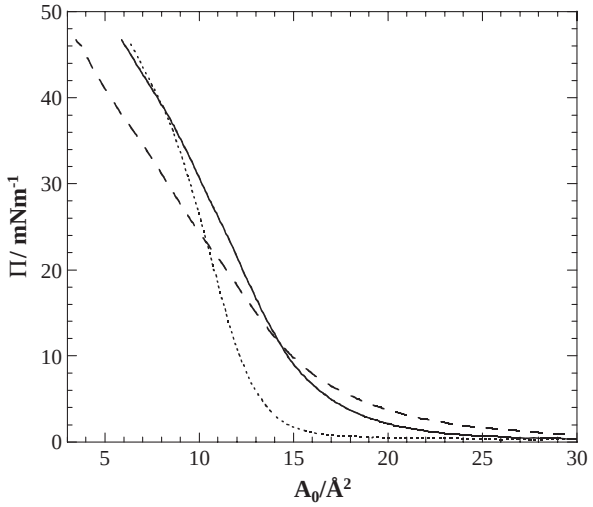

Fig. 4. Surface pressure compression isotherms of p-(Lys,Phe) spread on subphases with pH 3.5 (dashed trace), pH 8.1 (solid trace) and pH 10.2 (dotted trace). The subphase ionic strength was kept constant at 0.5 M by addition of NaCl.

As can be seen in Figs. 4 and 5, at large apparent mean molecular area, A_0 (≥15 $Å^2$) the surface pressure is increasing with decreasing pH and decreasing ionic strength. This is readily explained by the fact that the amount of charged polyamino acid monomers, and therefore the inter-and intra-molecular electrostatic repulsion, increase when lowering the pH. Decreasing the ionic strength increases the electrostatic repulsion and hence the surface pressure, in full agreement with previous results from surface studies on various charged di-block copolymers [33].

Using the standard procedure for derivation of A_0 at close packing (extrapolation of the linear part of the isotherm to Π=0), yield values between 13 and 18 $Å^2$ for p-(Lys,Phe),

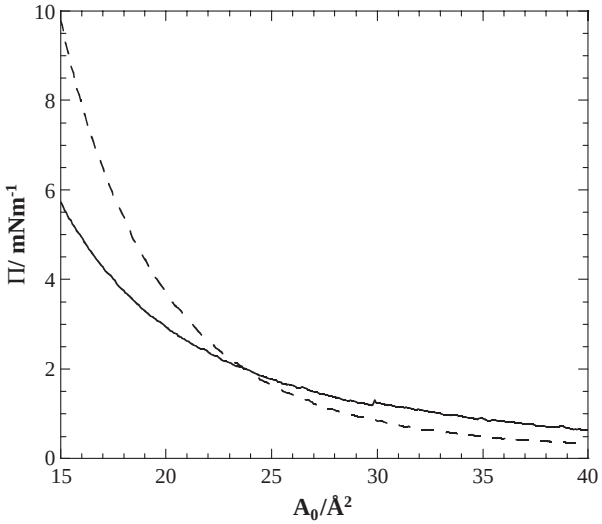

Fig. 5. Surface pressure compression isotherms of p-(Lys,Phe) spread on subphases with ionic strength of 0.1 M (solid trace) and 0.5 M (dashed trace) respectively. The subphase pH was 3.6±0.1.

depending on subphase pH and ionic strength (Fig. 4). These values are comparable to previously obtained values for hydrophobic α-helix forming polyamino acids at the air–water interface [27,34–39].

On subphases with pH≥8 an inflection point at $\Pi \approx 38$ mN m^{-1} is observed in the isotherm during compression (Fig. 4), whereas, during decompression, a shoulder is observed at $\Pi \approx 34$ mN m^{-1} (result nor shown). It is noteworthy that the isotherm of p-(Lys,Phe) does not display a more pronounced plateau in the compression isotherms, even at high pH where it is predominantly α-helical. This contrasts with entirely hydrophobic (non-titrating) α-helix forming polyamino acids studied at the air water interface, where a steep rise in the isotherm is generally followed by a flat plateau. The plateau is normally interpreted in terms of a collapse of a monolayer comprising close-packed α-helical rods and subsequent formation of a bi-or multi-layer [34,35]. Consequently, the absence of a collapse plateau for p-(Lys,Phe) indicates a lower degree of cooperativity or a slower kinetics of the collapse process. The electrostatic repulsion between the polyamino acid strands originating from the polyamino acid net charge and the presence of not only α-helix but also polyamino acid random coil conformation, could account for both these effects.

The Π vs. A_0 isotherm becomes steeper with higher pH, regardless of subphase ionic strength (Fig. 4). This can be explained by the larger flexibility of a peptide in random coil conformation (low pH), as compared with a peptide in α-helical conformation (high pH). In order to maximise the content of α-helix, attempts were done to investigate even higher subphase pH (0.1 M NaOH). However, these attempts were unsuccessful, since the peptide tended to adsorb irreversible to the edges of the trough, the barriers and the Wilhelmy plate. These problems were not observed at any other pH investigated.

LB films of p-(Lys,Phe), spread at the air–water interface at different pH and deposited on quartz, were investigated by means of circular dichroism (CD) spectroscopy. The general characteristics of the CD spectra of peptide LB films follow those of isotropic CD spectra of peptides in solutions [40,41]. However, previous works show that CD spectra of polyamino acid films containing laterally oriented polyamino acid strands comprise appreciable contributions from linear dichroism [27,35]. In analogy with these results, the CD spectrum of p-(Lys,Phe) displayed a distinct angular dependence, independent of pH, which thus implies a presence of laterally oriented p-(Lys,Phe) strands in all films (results not shown). When the samples were placed in a horizontal position, all spectra displayed a maximum at 192 nm, along with two minima at 208 and (less well-defined) 222 nm. These features are typical for a peptide in α-helical conformation (Fig. 6). As can bee seen in Fig. 6, p-(Lys,Phe) deposited from a subphase with pH 9, yields a markedly weaker spectra, though the typical characteristic contribution of a peptide in α-helix conformation is retained. However, deposition of films at pH≥9 proved very difficult. The transfer ratio during the deposition showed substantial variability (from 0.6 to 1.2) and it was difficult to prevent the surface pressure from rising. These problems is reflected in the fact that the overall transfer ratio at pH≥9.0 is 0.96, while the overall transfer ratio at pH<9 is appreciably higher (1.03–1.08). The difficulties encountered during deposition at high pH may be of electrostatic origin. At low pH, p-(Lys,Phe) and the quartz plate are oppositely charged, which of course facilitates deposition, while at higher pH, where p-(Lys,Phe) is uncharged, this electrostatic force is markedly reduced.

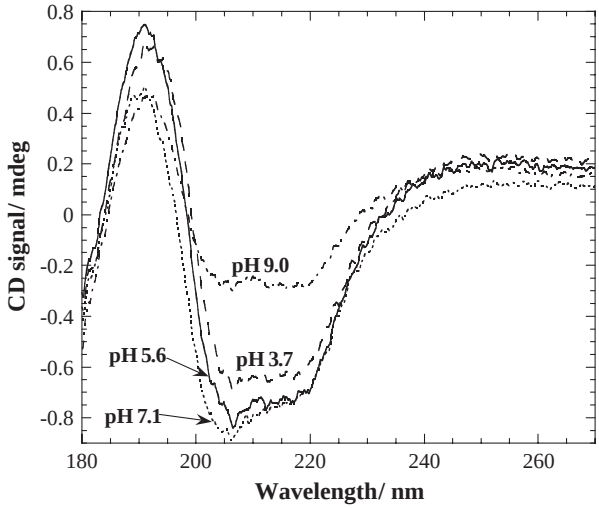

Fig. 6. CD spectra of LB films of p-(Lys,Phe) deposited on quartz at Π=18 mN m^{-1}. Prior to deposition, the polyamino acid was spread onto the air–water interface on four different subphase pH, namely pH 3.7 (dashed trace), pH 5.6 (solid trace), pH 7.1 (dotted trace) and pH 9.0 (dashed and dotted trace). The subphase ionic strength was kept constant at 0.1 M by addition of NaCl.

Random coil conformation gives only a weak CD signal in solution and this may reasonably be expected to hold true also for LB films. In combination with the presence of linear contributions to the CD spectra and the variable deposition, this makes quantitative determinations of the α-helix content in the peptide LB films impossible. However, appreciable amounts of β-sheet conformation would give a strong, characteristic contribution [34,35] and can consequently be ruled out. In other words, we may conclude that the LB films of p-(Lys,Phe) contain laterally oriented helices, but that the presence of random coil elements can not be verified, let alone quantified. The presence of α-helix conformation in LB films deposited also at low pH seems analogous to the behaviour of the peptide in solution. At low pH and an ionic strength of 0.1 M, the α-helix content of p-(Lys,Phe) in solution levels off at almost 20% in solution (Fig. 2). It therefore seems likely that the same conditions at the interface yield an α-helix content in the vicinity of 20%. Additionally, the fact that p-(Lys,Phe) is deposited on a oppositely charged quartz plate, increases the risk for surface rearrangement during deposition, and consequently,

an increased amount of α-helical structure on the plate compared to at the air–water interface before deposition, can not be ruled out. A viable, hydrophilic alternative to the quartz substrate is not available and a supplementary method in which α-helix and random coil conformation give equally strong response would obviously be very valuable when analysing the secondary peptide conformation in the LB-films. Unfortunately, no such method is available. Attenuated total reflection infrared spectroscopy (ATR-IR) and surface-enhanced Raman spectroscopy, which, in principle, would both be applicable, are ruled out due to band overlap [36,42].

To verify the presence of a proper surface monolayer of p-(Lys,Phe) at the air–water interface, LB films deposited from different subphase pH were investigated by means of atomic force microscopy (AFM; Fig. 7). Smooth monolayers were observed regardless of subphase pH. However, an increased presence of aggregates was observed with increasing pH. A similar aggregation behaviour, yielding more aggregates with higher pH, has previously been observed for an all α-helix, totally hydrophobic peptide [27]. In this previous investigation, the aggregates were shown to comprise trifluoroacetate crystallites, formed from TFA in the spreading solvent and deposited on top of the true polyamino acid monolayer. Since the aggregates do not contain any peptide, they have no influence on the CD spectra of deposited peptide films. Furthermore, they do not affect the behaviour of peptide monolayers, and no relationship whatsoever has been observed between the amount of aggregates and the peptide conformation.

Polyamino acids like p-(Lys,Phe) can, as a first approximation, be treated like a thread-or rod-like polyelectrolyte in terms of its surface arrangement. Therefore, in the semi-dilute regime (ca. 1–10 mN m^{-1}) [43] the surface pressure dependence of the surface concentration, Γ, would be expected to follow a power law and Γ to be inversely proportional to A_0 (Eq. (3)) [23,25,43–46].

$$\Pi \propto \Gamma^{y} \propto A_0^{-y} \tag{3}$$

Here, y is a critical exponent that gauges the thermodynamic conditions in the system [43,44]. In two dimensions y can be expressed as [23,25,43–45,47]

$$y = vd/(vd - 1) \tag{4}$$

where d is the space dimensionality (here d=2) and v is the two-dimensional Flory exponent, a critical exponent of the excluded area that makes it possible to express the molecular weight dependency of the peptide radius of gyration, R_g, in the form of $R_g \propto M_w^v$ [23,25,43–46]. Since v is directly related to the radius of gyration and its dependence of molecular mass, v provides information about the polymer conformation at the interface. It is trivial that v for a fully extended chain is unity, whereas the limiting v value for a polymer on a poor solvent is 0.5 [25]. Calculations show that v in a good solvent is 0.75–0.77 [44,45]. For a theta solvent the results from different calculations of the v exponent show larger variability (0.50–0.67), but the most recent calculations settle around v=0.57 [23,25,43–45].

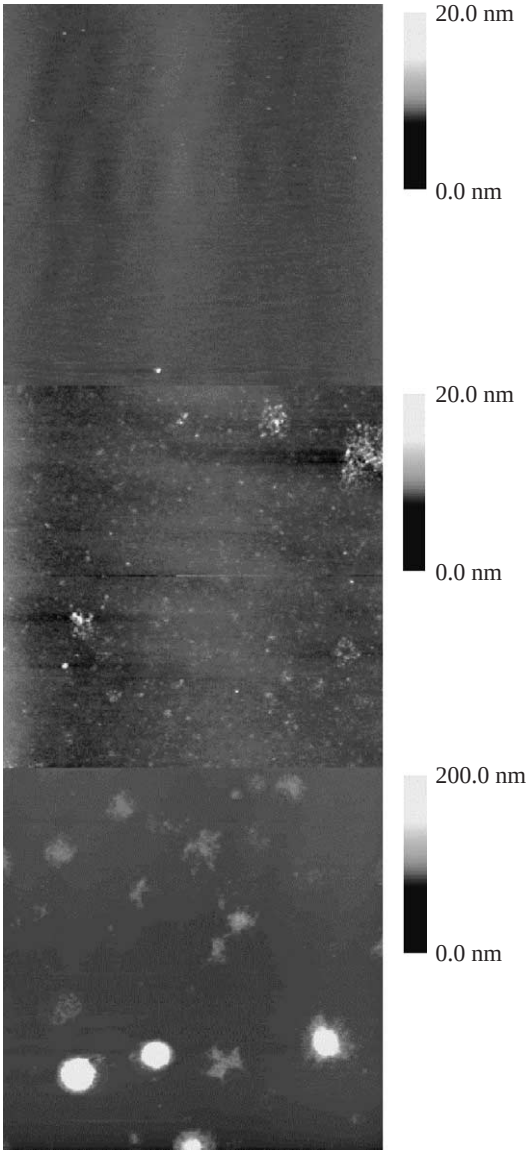

Fig. 7. AFM images of LB films of p-(Lys,Phe) spread on subphases with pH 5.6 (upper image), pH 9.0 (middle image) and pH 10.7 (bottom image). The ionic strength in all three cases was kept constant at 0.1 M by addition of NaCl. The films were deposited on mica at Π=18 mN m^{-1}. The dimensions of the displayed areas are 15×15 μm. Note that the z scale is ten times higher in the bottom image.

In principle, a plot of v as a function of subphase pH for a titrating peptide would yield a titration curve that describes its two-dimensional properties, thereby supplying indirect information about the peptide secondary conformation. A plot of Π vs. A_0 for p-(Lys,Phe) in a log–log scale (Fig. 8) indeed yields a linear region in the semi-dilute regime under all pH conditions, as predicted by Eq. (3). Using the slope ($-y$) of the linear region, v can be determined from Eq. (4). For p-(Lys,Phe) spread on a subphase with extremely low pH and low ionic strength

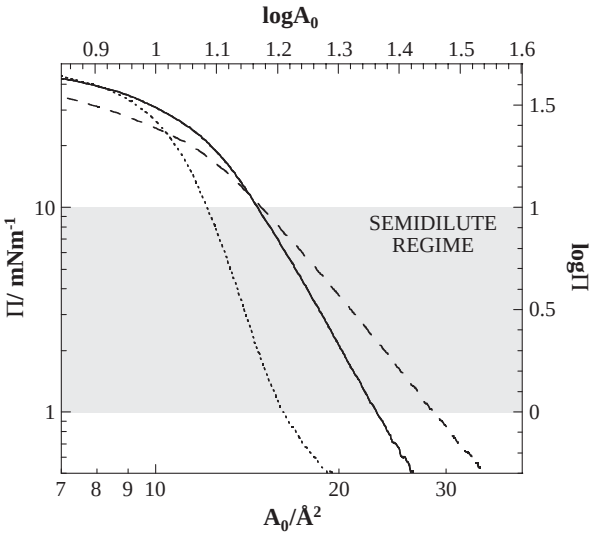

Fig. 8. Surface pressure as a function of the apparent mean molecular area for p-(Lys,Phe) spread on subphases with pH 3.5 (dashed trace), pH 8.1 (solid trace) and pH 10.2 (dotted trace). The subphase ionic strength was kept constant at 0.5 M.

(acetic acid, pH=3.0 and I=0.1 mM), ν is found to equal unity. This corresponds perfectly to the ν value of a fully stretched chain, and thus to the expected behaviour of a highly charged polyelectrolyte under conditions where there is substantial counter-ion condensation and little screening of the intra-molecular electrostatic repulsion. Increasing ionic strength at low pH is observed to lead to a decreasing value of ν. For the 0.1 and 0.5 M subphases, ν levels off at 0.93 and 0.71, respectively. Again, this is in agreement with expectation in the sense that increasing subphase ionic strength increases screening of the electrostatic repulsion, and simultaneously decreases the entropic loss originating from counter-ion condensation. These conditions yield a ν exponent closer to that of a peptide in a good solvent, in full agreement with the expected behaviour for a screened polyelectrolyte.

Increasing pH at constant ionic strength leads to a monotonous decrease of ν. At high pH, ν levels off at around 0.57 on both the 0.1 M and 0.5 M subphases. This value is deceptively close to the calculated value for a polymer under theta conditions. However, it has to be remembered that at high pH, where p-(Lys,Phe) is largely uncharged, the expected secondary conformation is all-helical. Long α-helices have a persistence length of 700–1400 Å, corresponding to 500–1000 amino acid residues in α-helix conformation [48–50]. For all practical purposes, these molecules behave as perfectly stiff rods, which, in turn, would seem to imply a ν value of unity. However, the derivation of ν presupposes that it is possible to identify a semi-dilute region in which the polymer strands are statistically distributed over the surface. Previous studies have shown that this picture is inapplicable to uncharged α-helices at the air–water interface, due to extensive peptide aggregation. More specifically, α-helical peptides form close-packed domains ("islands"), which partially covers the surface already at large A_0, i.e. at low surface pressures [27,51–54]. If each such domain is regarded a giant, disc-shaped polymer, we reach the conclusion that the expected ν value at high pH would rather be ca. 0.5. This follows directly from the observation the ν can be interpreted as the inverse of the (fractal) dimensionality of the polymer. This conclusion is lent strong experimental support by calculations of ν from our previous isotherm data on the helix-forming, hydrophobic peptides poly-L-leucine and poly-γ-methylglutamate [27,34,35]. These calculations give a ν value of 0.52, irrespective of polyamino acid molecular mass and subphase. The ν value in the present study at high pH (ν=0.57) thus strongly indicates that p-(Lys,Phe) is nearly all-helical under these conditions.

Previous, similar studies of β-casein (a protein known to be mostly in random coil conformation both in aqueous solutions and at interfaces) [23–26,55,56] have revealed an increase of ν with decreasing pH, similar to the one observed in the present study [24,25]. However, a more detailed comparison is difficult since the ionic strength in the β-casein studies was allowed to vary 50% or more during a series of experiment, whereas for p-(Lys,Phe) the subphase ionic strength is kept constant. Close to its isoelectric point, β-casein behaves in a different manner that p-(Lys,Phe), due to β-casein being net neutral, rather than totally uncharged. While ν is constant when varying the ionic strength for neutral p-(Lys,Phe) (high pH), ν increases with increasing salt for β-casein, just as would be expected for a polyampholyte.

The extraordinary good correlation between the calculated ν exponents and the expected surface behaviour of p-

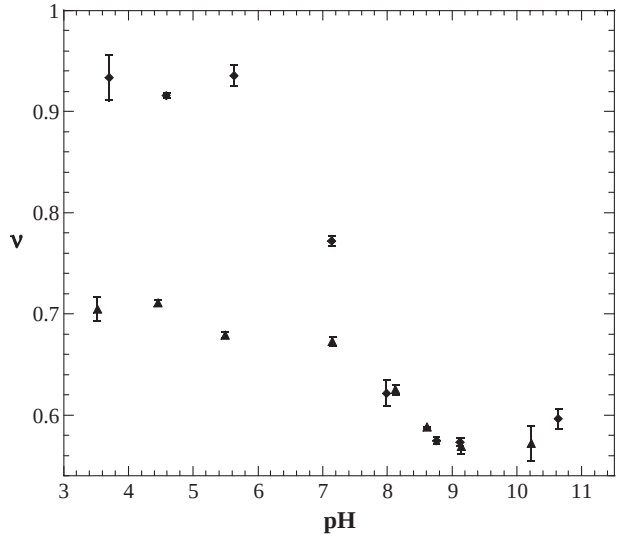

Fig. 9. The Flory exponent, ν (calculated from Eq. (4)) as a function of subphase pH for p-(Lys,Phe). The subphase ionic strength was kept constant at 0.1 M (diamonds) and 0.5 M (triangles) by addition of NaCl. The data points represent the mean value from at least three independent measurements at each pH, and the error bars correspond to one standard deviation.

(Lys,Phe) in α-helix and random coil conformation shows that by expressing v as a function of subphase pH, we have a method to estimate the surface conformation at the air–water interface.

3.3. Comparison of p-(Lys,Phe) in solution and at the interface

Comparison of the helix-to-coil transition in aqueous solution (Fig. 2) to the transition at the air–water interface (Fig. 9) shows that the titration curve midpoint is shifted drastically (ca. 2.5 pH units for I=0.1 M) towards lower pH for p-(Lys,Phe) at the air–water interfaced as compared to p-(Lys,Phe) aqueous solutions. One contributing factor to this shift is the fact that the apparent pK_a at the air–water interface differs from pK_a in solution [57]. Experiments have shown that for surfactants with –COOH or $–NH_2$ as head groups, pK_a shifts approximately 0.7 pH units at the surface, favouring the neutral species [58,59]. In addition the entropic loss, associated with α-helix formation, is less on the surface than in solution, due to the lower conformational and translational freedom in the 2-dimensional case, which would tend to favour formation of α-helix on the surface. Also, the α-helix has a strong dipole moment along the principal helix axis [60,61], and orientation of dipoles parallel to the surface would be expected to represent an energetic gain.

It has been shown earlier that p-Lys grafted to a surface has a markedly shifted titration curve midpoint (1.5 pH units) in comparison to free p-Lys [62], and the titration curve for co-poly-(glutamic acid, methylglutamate) (p-(Glu,MeGlu)) as determined by surface viscoelacticity and surface potential measurements, yields a titration curve midpoint 3.25 pH units higher (also favouring the neutral species) than pK_a for glutamate in solution [63]. The titration curve midpoint for p-(Lys,Phe) differs from pK_a for lysine in solution by 3.3 pH units, in excellent agreement with the previous p-(Glu,MeGlu) results.

4. Conclusions

In comparison to p-Lys in solution, p-(Lys,Phe) yield a wider random coil-to-α-helix transition, with a titration curve shifted towards lower pH. Addition of a non-ionic surfactant (β-$C_{12}G_2$) stabilises the α-helix conformation in p-(Lys,Phe) and prevents precipitation in the whole pH range investigated. At the air–water interface the peptide helix–coil transition can be followed by utilizing the Flory exponent, v. This method makes it possible to indirectly compare the helix–coil transition for p-(Lys,Phe) in solution with that at the air–water interface. The p-(Lys,Phe) titration curve midpoint at the interface is shifted approximately 2.5 pH units towards lower pH in comparison to the titration curve midpoint for p-(Lys,Phe) in solution. The latter conclusion is of relevance for conformation and conformational changes of membrane-transporting and membrane penetrating peptides as well as for the use of peptides in molecular devices.

Acknowledgment

Financial support from AstraZeneca R&D Lund and The Swedish Foundation for Strategic Research (Programme of Colloid and Interface Technology) is gratefully acknowledged. The authors thank Tommy Nylander for valuable and constructive discussions.

References

[1] J. Kurawaki, Y. Kusumoto, Potentiometric and spectroscopic characterization of copolypeptide-surfactant complexes formed by a cooperative binding system, J. Colloid Interface Sci. 225 (2000) 265–272.
[2] H. Saito, T. Ohki, M. Kodama, C. Nagata, Salt-induced conformational change of random copolymers $(Lys^{50}Tyr^{50})_n$ and $(Lys^{50}Phe^{50})_n$ studied by ^{1}H-and ^{13}C-nuclear magnetic resonances. Aggregation behavior of helical segments, Biopolymers 18 (1979) 1065–1072.
[3] G.D. Fasman, in: G.D. Fasman (Ed.), Factors Responsible for Conformational Stability, Poly-α-amino Acids: Protein Models for Conformational Studies, vol. 1, Marcel Dekker, New York, 1967, pp. 499–604.
[4] Y.P. Myer, The pH-induced helix–coil transition of poly-L-lysine and Poly-L-glutamic acid and the 238-mm dichroic band, Macromolecules 2 (1969) 624–628.
[5] A. Ciferri, D. Puett, L. Rajagh, J. Hermans, Potentiometric titrations and the helix–coil transition of poly-(L-glutamic acid) and poly-L-lysine in aqueous salt solutions, Biopolymers 6 (1968) 1019–1036.
[6] Y.N. Vorobjev, H.A. Scheraga, B. Honig, Theoretical modeling of electrostatic effects of titratable side-chain groups on protein conformation in a polar ionic solution. 2. pH induced helix–coil transition of poly(L-lysine) in water and methanol ionic solutions, J. Phys. Chem. 99 (1995) 7180–7187.
[7] A. Teramoto, H. Fujita, Statistical thermodynamic analysis of helix–coil transitions in polypeptides, J. Macromol. Sci., Rev. Macromol. Chem. C15 (1976) 165–278.
[8] Y.N. Vorobjev, H.A. Scheraga, B. Hitz, B. Honig, Theoretical modeling of electrostatic effects of titratable side-chain groups on protein conformation in a polar ionic solution. 1. Potential of mean force between charged lysine residues and titration of poly(L-lysine) in 95% methanol solution, J. Phys. Chem. 98 (1994) 10940–10948.
[9] F.T. Hesselink, T. Ooi, H.A. Scheraga, Conformational energy calculations. Thermodynamic parameters of the helix–coil transition for poly(L-lysine) in aqueous salt solution, Macromolecules 6 (1973) 541–552.
[10] E. Peggion, A.S. Verdini, A. Cosani, E. Scoffone, Conformational studies on polypeptides. Circular dichroism properties of random copolymers of lysine and phenylalanine in aqueous solutions an various pH values, Macromolecules 2 (1969) 194–198.
[11] M. Chittchang, H.H. Alur, A.K. Mitra, T.P. Johnston, Poly(L-lysine) as a model drug macromolecule with which to investigate secondary structure and membrane transport, Part I: physicochemical and stability studies, J. Pharm. Pharmacol. 54 (2002) 315–323.
[12] M. Chittchang, N. Salamat-Miller, H.H. Alur, D.G. Vander Velde, A.K. Mitra, T.P. Johnston, Poly(L-lysine) as a model drug macromolecule with which to investigate secondary structure and membrane transport, Part 2: diffusion studies, J. Pharm. Pharmacol. 54 (2002) 1497–1505.

[13] D. Bach, K. Rosenheck, R. Miller, Interaction of basic polypeptides with phospholipid vesicles: conformational study, Eur. J. Biochem. 53 (1975) 265–269.
[14] A. Shibata, S. Murata, S. Ueno, S. Liu, S. Futaki, Y. Baba, Synthetic copoly(Lys,Phe) and poly(Lys) translocate through lipid bilayer membranes, Biochim. Biophys. Acta 1616 (2003) 147–155.
[15] R.M. Santelle, H. Jei Li, Studies on interaction between poly(L-lysine[58], L-phenylalanine[42]) and deoxyribonucleic acids, Biochemistry 14 (1975) 3604–3611.
[16] A. El-Aneed, An overview of current delivery systems in cancer gene therapy, J. Control. Release 94 (2004) 1–14.
[17] A.C. Roche, I. Fajac, S. Grosse, N. Frison, C. Rondanino, R. Mayer, M. Monsigny, Glycofection: facilitated gene transfer by cationic glycopolymers, Cell. Mol. Life Sci. 60 (2003) 288–297.
[18] D.T. Klink, M.C. Glick, T.F. Scanlin, Gene therapy of cystic fibrosis (CF) airways: a review emphasizing targeting with lactose, Glycoconj. J. 18 (2001) 731–740.
[19] J. Kim, H. Kim, Fusion of negatively charged phospholipid vesicles mediated by polyarginine and copolymers of lysine and hydrophobic amino acids, Kor. Biochem. J. 18 (1985) 403–409.
[20] K. Fukushima, T. Inoue, R. Shimozawa, CD spectral change of lysine-phenylalanine random copolymer induced by phosphatidylecholine vesicles, Fukuoka Univ. Sci. Rep. 21 (1991) 211–217.
[21] T. Nylander, in: M. Malmsten (Ed.), Protein Adsorption in Relation to Solution Association and Aggregation, Biopolymers at Interfaces, vol. 110, Marcel Dekker, Inc., New York, 2003, pp. 259–294.
[22] W. Norde, C.E. Giacomelli, Conformational changes in proteins at interfaces: from solution to the interface and back, Macromol. Symp. 145 (1999) 125–126.
[23] M. Mellema, D.C. Clark, F.A. Husband, A.R. Mackie, Properties of β-casein at the air/water interface as supported by surface rheological measurements, Langmuir 14 (1998) 1753–1758.
[24] P. Cicuta, I. Hopkinson, P.G. Petrov, Protocol of protein conformation in a langmuir monolayer, J. Chem. Phys. 115 (2001) 9991–9994.
[25] P. Cicuta, I. Hopkinson, Studies of a weak polyampholyte at the air–buffer interface: the effect of varying pH and ionic strength, J. Chem. Phys. 114 (2001) 8659–8670.
[26] P.W.J.R. Caessens, H.H.J. De Jongh, W. Norde, H. Gruppen, The adsorption-induced secondary structure of β-casein and of distinct parts of its sequence in relation to foam and emulsion properties, Biochim. Biophys. Acta 1430 (1999) 73–83.
[27] H. Sjögren, S. Ulvenlund, Effects of pH, ionic strength, calcium and molecular mass on the arrangement of hydrophobic peptide helices at the air–water interface, J. Phys. Chem., B 108 (2004) 20219–20227.
[28] N. Greenfield, G.D. Fasman, Computed circular dichroism spectra for the evaluation of protein conformation, Biochemistry 8 (1969) 4108–4116.
[29] Handbook of Chemistry and Physics, CRC Press, Inc., Boca Raton, 2004.
[30] A.J. Doig, Recent advances in helix–coil theory, Biophys. Chemist. 101–102 (2002) 281–293.
[31] S. Nilsson, W. Zhang, Helix–coil transitions of a titrating polyelectrolyte analysed within the poisson–bolzmann cell model. Effects of pH and salt concentrations, Macromolecules 23 (1990) 5234–5239.
[32] W. Zhang, S. Nilsson, Helix–coil transition of a titrating polyelectrolyte analyzed within the poisson–boltzmann cell model. Effects of pH and counterion valency, Macromolecules 26 (1993) 2866–2870.
[33] E. Bringuier, R. Vilanove, Y. Gallot, J. Selb, F. Rondelez, Surface pressure of charged di-block copolymer films at an air–water interface, J. Colloid Interface Sci. 104 (1985) 95–106.
[34] S. Ulvenlund, H. Gillgren, A. Stenstam, P. Bäckman, E. Sparr, Hydrophobic homopolymers of native α-L-amino acids at the air–water interface. A study by circular dichroism spectroscopy, atomic force microscopy and surface balance experiments, J. Colloid Interface Sci. 242 (2001) 346–353.
[35] H. Gillgren, A. Stenstam, M. Ardhammar, B. Nordén, E. Sparr, S. Ulvenlund, Morphology and molecular conformation in thin films of poly-γ-methyl-L-glutamate at the air–water interface, Langmuir 18 (2002) 462–469.
[36] G.I. Loeb, R.E. Baier, Spectroscopic analysis of polypeptide conformation in polymethylglutamate monolayers, J. Colloid Interface Sci. 27 (1968) 38–45.
[37] B.R. Malcolm, Hydrophobic side chain interactions in synthetic polypeptides and proteins at the air–water interface, in: R.E. Baier (Ed.), Applied Chemistry at Protein Interfaces, Adv. Chem. Ser., vol. 145, 1975, pp. 338–359.
[38] G.D. Fasman, Monolayer studies of synthetic poly (α-amino acids), Mater. Res. Soc. Symp. Proc. 218 (1991) 49–55.
[39] P. Lavigne, P. Tancréde, F. Larmarche, J.-J. Max, Packing of hydrophobic α-helices: a study at the air–water interface, Langmuir 8 (1992) 1988–1993.
[40] A. Rodger, B. Nordén, Circular Dichroism and Linear Dichroism, Oxford University Press, New York, 1997.
[41] L. Stevens, R. Townend, S.N. Timasheff, G.D. Fasman, J. Potter, The circular dichroism of polypeptide films, Biochemistry 7 (1988) 3717–3720.
[42] J.L. Koenig, Raman spectroscopy of biological molecules: a review, J. Polym. Sci., Part D: Macromol. Rev. 6 (1972) 59–177.
[43] R. Myrvold, F.K. Hansen, B. Balinov, R. Skurtveit, Monolayers of some poly(oxyethylene)-based surfactants at the air–water interface: the effect of structural variations and salt concentration, J. Colloid Interface Sci. 215 (1999) 409–419.
[44] Q. Jiang, Y.C. Chiew, Determination of the ν exponent for soluble polymeric monolayers at an air/water interface, Macromolecules 27 (1994) 32–34.
[45] R. Vilanove, D. Poupinet, F. Rondelez, A critical look at measurements of the ν exponent for polymer chains in two dimensions, Macromolecules 21 (1988) 2880–2887.
[46] P.G. de Gennes, Scaling Consepts in Polymer Physics, Cornell Univ. Press Ltd., London, 1979.
[47] E.P.K. Currie, A.B. Sieval, G.J. Fleer, M.A. Cohen Stuart, Polyacrylic acid brushes: surface pressure and salt-induced swelling, Langmuir 16 (2000) 8324–8333.
[48] M. Schmidt, Combined integrated and dynamic light scattering by poly(γ-benzyl glutamate) in a helicogenic solvent, Macromolecules 17 (1984) 553–560.
[49] J. Helfrich, R. Hentschke, U.M. Apel, Molecular dynamics simulation study of poly(γ-benzyl L-glutamate) in dimethylformamide, Macromolecules 27 (1994) 472–482.
[50] H. Block, E.F. Hayes, A.M. North, Dielectric behaviour of solutions of poly-γ-benzyl-L-glutamate and of copolymers with the D-enantiomorph, Trans. Faraday Soc. 66 (1970) 1095–1105.
[51] M. Fukuto, R.K. Heilmann, P.S. Pershan, S.M. Yu, J.A. Griffiths, D.A. Tirrell, Structure of Poly(γ-benzyl-L-glutamate) monolayers at the gas–water interface: a brewster angle microscopy and x-ray scattering study, J. Chem. Phys. 111 (1999) 9761–9777.
[52] B.R. Malcolm, Molecular structure and deuterium exchange in monolayers of synthetic polypeptides, Proc. R. Soc., A 305 (1968) 363–385.
[53] R.L. Shuler, W.A. Zisman, A study of films of poly(γ-methyl L-glutamate) adsorbed on water using wave damping and other methods, Macromolecules 5 (1972) 487–492.
[54] P. Lavigne, P. Tancréde, F. Lamarche, M. Grandbois, C. Salesse, The organization of poly-γ-benzyl-L-glutamate in the α-helix conformation at the air–water interface, Thin Solid Films 242 (1994) 229–233.
[55] E. Dickinson, D.S. Horne, J.S. Phipps, R.M. Richardson, A neutron refelctivity study of the adsorption of β-casein at fluid interfaces, Langmuir 9 (1993) 242–248.
[56] A.R. Mackie, J. Mingins, A.N. North, Characterisation of adsorbed layers of a disordered coil protein on polystyrene latex, J. Chem. Soc., Faraday Trans. 87 (1991) 3043–3049.
[57] M. Gouy, Sur la constitution de la charge électrique a la surface d'un électerolyte, J. Phys. 9 (1910) 457–468.

[58] P. Dynarowicz-Latka, A. Dhanabalan, O.N. Oliveira Jr., Modern physicochemical research on langmuir monolayers, Adv. Colloid Interface Sci. 91 (2001) 221–293.
[59] P. Dynarowicz-Latka, A. Cavalli, O.N. Oliveira Jr., Dissociation constants of aromatic carboxylic acids at the air/water interface, Thin Solid Films 360 (2000) 261–267.
[60] C.R. Cantor, P.R. Schimmel, Biophysical chemistry Part III: The Behaviour of Biological Macromolecules, W.H. Freeman & Co., New York, 1980.
[61] A. Wada, in: M.A. Stahmann (Ed.), Chain Regularity and Dielectric Properties of Poly-α-amino Acids in Solution, Polyamino Acids, Polypeptides, and Proteins, The University of Wisconsin Press, Wisconsin, 1962, pp. 131–146.
[62] Y. Wang, Y.C. Chang, Synthesis and conformational transition of surface-tethered polypeptide: poly(L-lysine), Macromolecules 36 (2003) 6511–6518.
[63] J. Caspers, C. Berliner, J.-M. Ruysschaert, J. Jaffe, Conformation of a copolypeptide at the air–water interface, J. Colloid Interface Sci. 49 (1974) 433–441.